Journal of Alloys and Compounds 293–295 (1999) 484–489

# In situ study of hydriding–dehydriding properties in some Pd/Mg thin films with different degree of Mg crystallization

K. Higuchi[a,*], H. Kajioka[a], K. Toiyama[a], H. Fujii[b], S. Orimo[b,1], Y. Kikuchi[c]

[a]*Western Hiroshima Prefecture Industrial Research Institute, Kure, 737-0004, Japan*
[b]*Faculty of Integrated Arts and Sciences, Hiroshima University, Higashi-Hiroshima, 739-8521, Japan*
[c]*ULVAC JAPAN, Ltd., Chigasaki, 253-0071, Japan*

---

## Abstract

A new in situ system with the functions of thin film formation and analysis of hydrogen absorption–desorption properties has been developed to clarify hydrogen storage properties in nano-scaled composites. In this work, some Pd/Mg films (Pd (25 nm)-coated Mg (200 nm) films) with different degree of crystallization in the Mg layer were prepared in different sputtering conditions by changing RF coil powers and argon pressures. Hydrogenation under hydrogen gas pressure of 0.1 MPa at 373 K for 24 h indicated that $MgH_2$ and non-crystalline Mg hydrides were formed in all the Pd/Mg films and the hydrogen content reached 2.9~6.6 mass% independent of the degree of Mg crystallization. From the thermal desorption spectrum, it was deduced that the dehydriding temperature decreased with decreasing the degree of crystallization in the Mg layer in Pd/Mg films and the Pd/Mg film with lowest crystallization absorbed 5.6 mass% of hydrogen and all the hydrogen desorbed at a temperature lower than 463 K in vacuum.

*Keywords:* Thin film; Magnesium; Palladium; Hydrogen storage; Sputtering; Crystallinity

---

## 1. Introduction

Hydrogen absorbing alloys are promising as functional materials for hydrogen batteries, hydrogen and thermal storage, and heat pumps. Many searching studies of new alloys have been done for developing new high-performance hydrogen storage materials that desorb hydrogen at temperatures lower than 373 K and have more than 3 mass% hydrogen capacity. As one of the methods for synthesizing the high-performance alloys, we propose to make two kinds of the alloys/metals with different hydrogen storage properties into composite in nano-meter scale, because advantageous hydriding–dehydriding properties in both materials are extracted through elastic interactions in between nano-sublattices. One is a metal/alloy with high hydrogen absorbed capacity but high temperature desorbing temperature, while the other is that with just the opposite properties. For instance, the former is Mg and the later is Pd or $LaNi_5$. Especially, Mg is very much attractive as one of the hydrogen storage materials because of having a very high capacity of 7.6 mass% in $MgH_2$.

To clarify this point, we have developed a new in situ system with the functions of thin film formation and analysis of hydrogen absorption–desorption properties under high vacuum without exposing in air. Thin film is the most suitable for synthesizing the nano-scaled composites because we can control well interface, thickness, composition and degree of crystallization.

Thin films for hydrogen storage have been studied so far [1–6]. Krozer et al. have reported unusual kinetics of the hydrogen uptake on the Pd/Mg film that the saturation hydrogen content decreases with increasing $H_2$-gas pressures. This result has been explained in terms of formation of the $MgH_2$ at the Pd/Mg interface, which blocks hydrogen diffusion [1]. The $LaNi_5$ film has been investigated for application to electrodes of batteries [6], in which the crystalline film has a higher capacity than the amorphous film but has a lower capacity than the bulk alloy. However, the relationships between the structural and hydrogenation properties in thin films have not been studied yet in detail.

In this paper, we describe the outline of the new in situ system, present our results of hydriding–dehydriding prop-

---

*Corresponding author. Tel.: +81-823-74-0050; fax: +81-823-74-1131.

[1] Present address: Max-Planck Institute für Metallforschung, Institute für Physik, Heisenbergstrasset, 70569 Stuttgart, Germany.

0925-8388/99/$ – see front matter
PII: S0925-8388(99)00470-3

erties of the Pd-coated Mg film (Pd/Mg film) with different degree of Mg crystallization, and discuss whether some advantageous properties are extracted or not in nano-composite Pd/Mg films.

## 2. Experimental details

### 2.1. Outline of the in situ system

A schematic diagram of the in situ system with the functions of film formation and analysis of hydrogen absorption–desorption properties is shown in Fig. 1. The system consists of three units. The center unit is a sputtering chamber, the right one is a hydriding chamber and the left one is an analysis chamber for evaluating dehydriding properties. The substrate in the holder can be moved among the three units with two magnetic manipulators. The residual gas pressure in this system can be kept at the order of $10^{-5}$ Pa. Three RF associated magnetron sputtering units [7] are set in the sputtering chamber. The main features of the sputtering unit with RF coil just above the target are that (1) sputtering can be realized even at the argon (Ar) pressure of $7.0\times1.0^{-2}$ Pa, because ionization of Ar and metal is strongly facilitated, and (2) RF coil power can be independently controlled for D.C. power. The targets are tilted 30° from the perpendicular axis of the substrate and the target-to-substrate distance is 153 mm.

The hydrogenation of thin films can be performed in the hydriding chamber. The chamber can be heated up to 773 K from room temperature by a mantle heater, and hydrogen gas can be introduced up to a pressure of 0.2 MPa.

The analysis chamber of dehydriding properties consists of the upstream and downstream rooms. The orifice of 30 $l\,s^{-1}$ is located between both the rooms. The upstream room with a molybdenum-heater and a pressure gauge is also used for the sample introducing room. A mass spectrometer and a pressure gauge are set at the down-stream room. The amount of desorbed hydrogen gas from the sample is measured by mass spectroscopy method and through put (orifice) methods in the heating process of the sample, which is called a thermal desorption spectroscopy (TDS) method [8].

Table 1
Sputtering condition and deposition rate of the Mg layer

| Condition | (I) | (II) | (III) | (IV) |
|---|---|---|---|---|
| Ar pressure (Pa) | $7.0\times10^{-2}$ | $7.0\times10^{-2}$ | $7.0\times10^{-1}$ | $7.0\times10^{-1}$ |
| RF coil power (W) | 0 | 100 | 0 | 200 |
| D.C. current (A) | 0.05 | 0.05 | 0.05 | 0.05 |
| Deposition rate ($nm\,s^{-1}$) | 0.13 | 0.13 | 0.04 | 0.08 |

### 2.2. Film preparation

The Pd/Mg films were prepared on the glass substrate (Corning #7059 20×20×0.5 mm) by the RF associated magnetron sputtering at room temperature. Before sputtering, the sputtering chamber was baked out and the residual gas pressure was kept at the order of $10^{-7}$ Pa. The Mg and Pd targets with 4 N purity and the Ar gas with 6 N purity were used for the sputtering. Mg films ((A),(B),(C) and (D)) are prepared under Mg sputtering conditions ((I), (II), (III) and (IV)) given in Table 1, respectively, and their deposition rates are also shown in Table 1. The Pd film was prepared at the Ar pressure of $7.0\times10^{-2}$ Pa with a target D.C. current of 0.10 A and the RF coil power of 50 W, and the deposition rate was 0.22 $nm\,s^{-1}$. The Pd/Mg films ((a), (b), (c) and (d)) are prepared by coating with the Pd layer on Mg films ((A),(B),(C) and (D)), respectively. Mg layers are 200 nm and Pd layers are 25 nm thick in the Pd/Mg films.

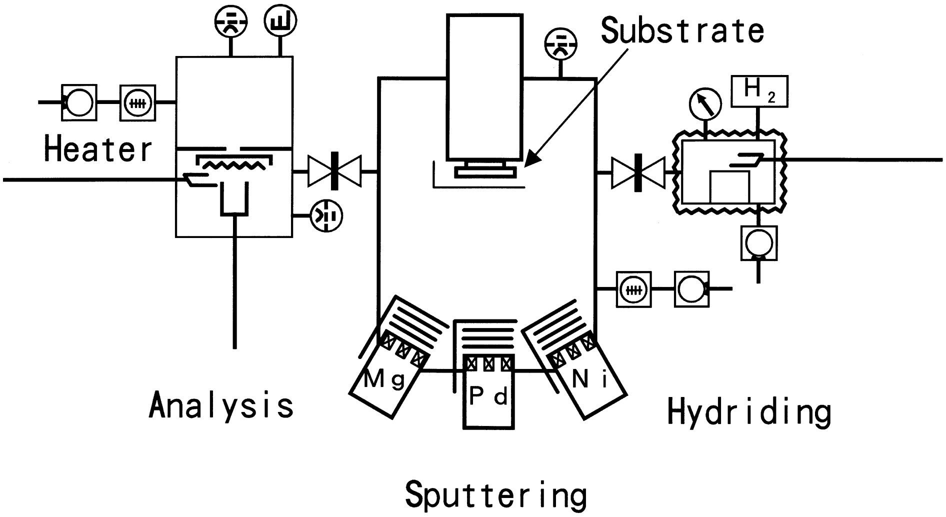

Fig. 1. A schematic diagram of the new in situ system with the functions of thin film formation and analysis of hydrogen absorption–desorption properties.

After film formation, the Pd/Mg films were hydrogenated at 373 K for 24 h, and the dehydriding properties were examined by TDS-analysis in the heating process at 4 K $\mathrm{min}^{-1}$ up to 773 K from room temperature.

The film thickness was measured by a surface-measuring instrument. The degree of crystallization of the films were characterized by the X-ray diffraction method using Cu Kα radiation. The morphologies of the Mg and Pd films were observed by a scanning electron microscope (SEM).

## 3. Results and discussion

### 3.1. Formation of Mg, Pd and Pd/Mg films

Prior to formation of the Pd/Mg films, the Mg films with 200 nm and Pd film with 100 nm in thickness were prepared. The SEM images for the top surface of these films are shown in Fig. 2, together with that of the Pd film. All the Mg films and Pd film are very smooth and compact. The appearance of all the films is mirror-like the same as the glass substrate. These morphologies correspond to Zone-T of the structure zone model proposed by Thornton [9]. This suggests that the interface of the Pd/Mg film is so flat and comfortable that hydrogen can easily transfer at the interface.

The X-ray diffraction profiles of Pd/Mg films ((a), (b), (c) and (d)) are shown in Fig. 3, together with that of the glass substrate as background. The profiles of Pd/Mg films reveal the (002) preferred orientation for Mg films, but no preferential orientation for the Pd layer on the Mg films. It should be noted that the preferential orientation of the *c*-axis in the Pd/Mg films is not affected by the Ar pressure and RF power. However, the Mg (002) peak intensity is dramatically changed by the sputtering conditions, while the full width at half maximum is almost the same as ca. 0.23 (π/180) radian for all the Pd/Mg films. The Mg (002) peak intensity is lower at the Ar pressure of $7.0\times10^{-1}$ Pa than $7.0\times10^{-2}$ Pa with no RF coil power, indicating that the degree of Mg crystallization decreases with increasing Ar pressure with no RF power. At the high

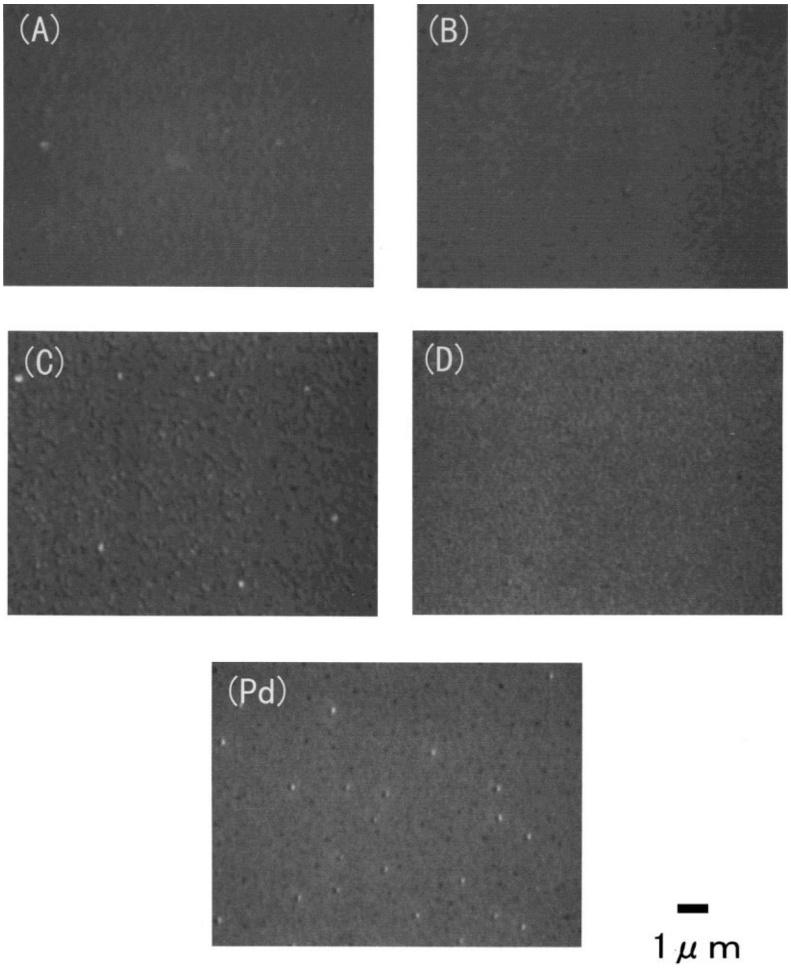

Fig. 2. SEM images for the top surface of the Mg films ((A), (B), (C) and (D)) and Pd film (Pd). Mg films ((A), (B), (C) and (D)) were prepared under the sputtering conditions ((I), (II), (III) and (IV)) in Table 1, respectively. The Pd film was prepared at the Ar pressure of $7.0\times10^{-2}$ Pa with a target D.C. current of 0.10 A and RF coil power of 50 W.

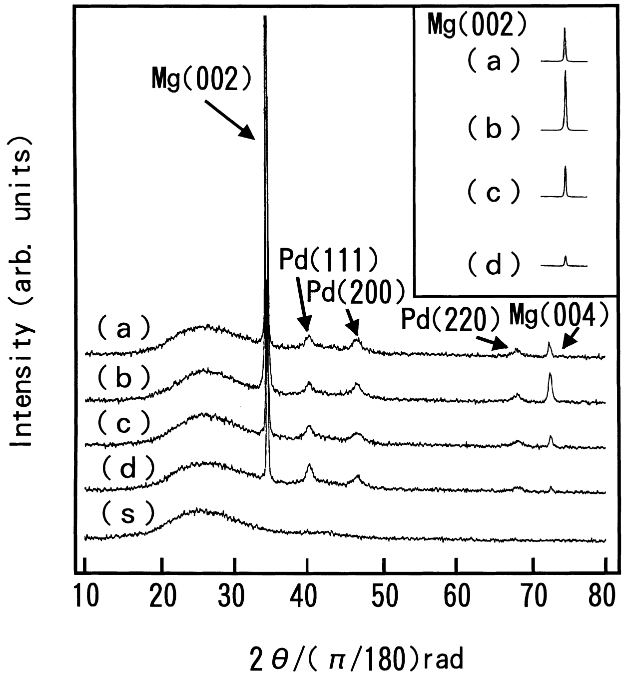

Fig. 3. X-ray diffraction profiles of the Pd/Mg films ((a), (b), (c) and (d)) before hydrogenation and glass substrate (s). Mg layers of these films ((a), (b), (c) and (d)) were prepared under the sputtering conditions ((I), (II), (III) and (IV)) in Table 1, respectively, and coated by the Pd layer under the same conditions as in Fig. 2.

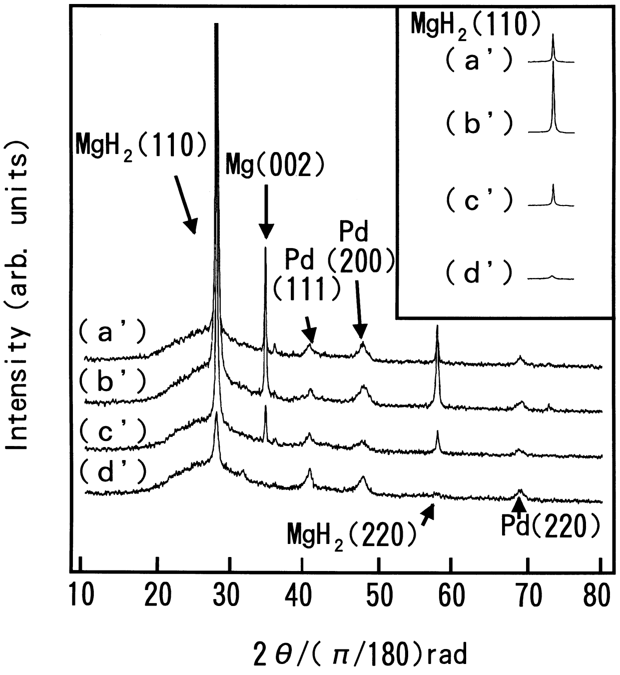

Fig. 4. X-ray diffraction profiles of the hydriding Pd/Mg films ((a′), (b′), (c′) and (d′)) at 373 K for 24 h. These films were prepared under the same conditions ((a), (b), (c) and (d)) as in Fig. 3, respectively.

Ar-pressure, the Mg (002) peak intensity decreases drastically with increasing RF coil power.

### 3.2. Hydrogenation of Pd/Mg films

The X-ray diffraction profiles of the Pd/Mg films after hydrogenation are shown in Fig. 4. These films are not the same as those in Fig. 3, but have been prepared under the same sputtering conditions and hydrogenated. The interesting points are summarized as follows: (1) The (110) peak of $MgH_2$ becomes significant after hydrogenation, but the Mg (002) peak still exists except for the film (d). This suggests that $MgH_2$ has been formed in the upper part but not formed at the bottom part of the Mg layer in the Pd/Mg films. (2) The Mg (002) peak position in Fig. 4 does not change after hydrogenation, indicating that no hydrogen is soluble in the hcp-Mg lattice. This supports the model that the Mg hydride begins to grow from the interface between Pd and Mg and the $MgH_2$ hydride layer grows into the Mg layer [5]. (3) The $MgH_2$ (110) peak intensities of (a′), (b′), (c′) and (d′) in Fig. 4 are almost proportional to those of the Mg (002) peak intensities of (a), (b), (c) and (d) in Fig. 3, respectively. This suggests that the structure change from the hcp-structure of Mg to the rutile one of $MgH_2$ occurs so as to minimize the average transfer distance of Mg atoms. At this transformation, the relationship between the crystalline orientations such that the Mg (002) direction corresponds to the $MgH_2$ (110) direction could be realized. (4) The X-ray peak positions of the Pd layers in (a′), (b′), (c′) and (d′) do not change from the corresponding ones in Fig. 3, and the X-ray peak of the Pd hydride is not observed. It seems that hydrogen in the Pd layer has been completely desorbed, since the hydriding Pd/Mg films have been kept in vacuum at once before X-ray examination. (5) On the other hand, the non-Pd-coated Mg film did not absorb hydrogen at all even in the same hydriding condition (at 373 K under 0.1 MPa $H_2$-gas atmosphere). This confirms that Pd acts as a catalyst for dissociating the hydrogen molecule into protium (hydrogen atom).

### 3.3. Dehydriding properties of Pd/Mg films

TDS spectra of the hydriding Pd/Mg films are shown in Fig. 5. These films are not the same as those in Fig. 4, but the preparation conditions are the same. The shape of the spectra with a small peak at low temperature and a large peak at high temperature is similar for all the films. However, the peak position of TDS spectra depends on the Mg sputtering conditions. The start and end points of hydrogen desorption temperatures are summarized in Table 2, together with the integrated value of ion current ($m/e = 2$) and total hydrogen content H/Mg (mass%). These dehydriding temperatures are much lower than that of pure Mg [10], but are close to those obtained in the hydriding Pd/Mg films with $\alpha+\beta$ phases by Krozer et al. [2]. The small peak at lower temperature might be due to desorption of hydrogen in the interface boundary between Pd and

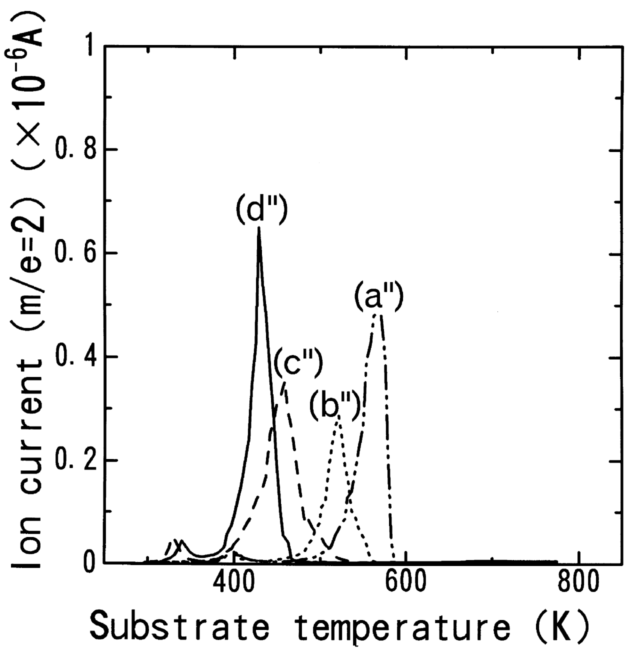

Fig. 5. TDS spectra of the hydriding Pd/Mg films ((a″), (b″), (c″) and (d″)). These films were prepared under the same conditions ((a′), (b′), (c′) and (d′)) as in Fig. 4, respectively.

Mg. The total hydrogen contents (H/Mg) in the hydriding Pd/Mg films are between 2.9 and 6.6 mass%, and these do not correspond to the peak intensities of $MgH_2$ in the X-ray profiles. This indicates that non-crystalline Mg hydride with no X-ray diffraction peak, i.e. amorphous-like Mg hydride, is formed in the Pd/Mg films with the weak Mg (002) peak intensity. We believe that since hydrogen can be easily soluble in the amorphous phase, the amorphous hydride might be usually more unstable than the crystal hydride. The amorphous-like Mg hydride is found to desorb hydrogen at lower temperatures than that of crystalline $MgH_2$, as is shown in Fig. 5(c″) and (d″). From the above experimental results, we conclude that the high hydrogen content and low hydriding–dehydriding temperature in the Pd/Mg film with the lowest degree of Mg crystallization gives proof of the possibility to extract some advantageous properties of Mg and Pd itself in the nano-scaled films. The hydriding–dehydriding properties obtained in the Pd/Mg film (d) are very close to the goal of NEDO for practical use of hydrogen storage material which can be used at a temperature lower than 373 K and have more than 3 mass% hydrogen capacity.

Table 2
Dehydriding properties of the hydriding Pd/Mg films[a]

| Sample | (a″) | (b″) | (c″) | (d″) |
|---|---|---|---|---|
| $T_d$ (K) | 383~583 | 353~563 | 313~533 | 313~463 |
| $I_{m/e=2}$ (A·S) | $2.68\times10^{-4}$ | $1.62\times10^{-4}$ | $2.53\times10^{-4}$ | $2.78\times10^{-4}$ |
| H/Mg (mass%) | 5.3 | 2.9 | 6.6 | 5.6 |

[a] $T_d$: Range of hydrogen desorption temperature, $I_{m/e=2}$: Integrated value of ion current ($m/e = 2$).

Finally, we describe about durability. After dehydriding the hydriding Pd/Mg film (d′) by heating to 473 K using TDS method, the same film was hydrogenated again in the hydriding chamber at the same conditions and was examined by TDS method again. The second TDS profile was similar to the first TDS profile. This suggests that the hydriding–dehydriding cycles in the Pd/Mg films (d) can be reproduced at a lower temperature than 473 K.

## 4. Summary

We have developed the new in situ system with the functions of thin film formation and analysis of hydriding–dehydriding properties. Using this system, we prepared four kinds of Pd/Mg films with different RF sputtering conditions and examined hydriding–dehydriding properties in the temperature range from room temperature to 773 K. The results obtained are summarized as follows.

1. The profiles of Pd/Mg films reveal the (002) preferred orientation for the Mg films. The Mg (002) peak intensity can be controlled by the sputtering conditions.
2. The $MgH_2$ (110) peak intensity in the hydriding Pd/Mg films correlates to the Mg (002) peak intensity in the pre-hydriding Pd/Mg films.
3. The dehydriding temperature is strongly affected by the degree of Mg crystallization, while the hydrogen capacity in the Mg layer is not. The dehydriding temperature becomes lower as much as the degree of Mg crystallization for the Pd/Mg films decrease.
4. The advantageous properties of Pd and Mg itself for hydrogen storage can be extracted in the nano-composite Pd/Mg films with the lowest degree of Mg crystallization, and the resultant hydriding–dehydriding properties are close to the goal of NEDO for the practical use of hydrogen storage material.
5. Hydriding–dehydriding cycles in the Pd/Mg film with the lowest degree of Mg crystallization can be reproduced for lower temperatures than 473 K.

## Acknowledgements

This work was supported by the Research Development Corporation of Japan and Hiroshima Prefecture and the Proposal-Based New Industry Creative Type Technology R&D Promotion Program from the New Energy and Industrial Technology Development Organization (NEDO) of Japan. This research was mainly investigated at Hiroshima Prefecture Joint Research Center for Advanced Technology in Higashi-Hiroshima city.

## References

[1] A. Krozer, B. Kasemo, J. Vac. Sci. Technol. A5 (1987) 1003.

[2] A. Krozer, B. Kasemo, J. Less-Common Metals 160 (1990) 323.

[3] A. Fischer, H. Köstler, L. Schlapbach, J. Less-Common Metals 172–174 (1991) 808.

[4] A. Fischer, A. Krozer, L. Schlapbach, Surface Sci. 269–270 (1992) 737.

[5] P. Spatz, H.A. Aebischer, A. Krozer, L. Schlapbach, Z. Phys. Chem., Bd. 181 S393–S397 (1993) 955.

[6] T. Sakai, H. Ishikawa, H. Miyamura, N. Kuriyama, J. Electrochem. Soc. 138 (1991) 908.

[7] M. Mastuura, T. Yamamoto, T. Morita, T. Kurauchi, J. Vac. Soc. Jpn. (in Japanese) 41 (1998) 147.

[8] N. Hirashita, S. Tokitoh, H. Uchida, Jpn. J. Appl. Phys. 32 (1993) 1787.

[9] J.A. Thornton, Ann. Rev. Mater. Sci. 7 (1977) 239.

[10] P. Selvam, B. Viswanathan, C.S. Swamy, V. Srinivasan, Int. J. Hydrogen Energy 13 (1988) 87.